Journal of Materials Chemistry C

PAPER

View Article Online
View Journal | View Issue

Check for updates

Cite this: J. Mater. Chem. C, 2017, 5, 6563

Towards enhancing spin states in doped arylamine compounds through extended planarity of the spin coupling moieties†

Łukasz Skórka,[a] Jean-Marie Mouesca,[bc] Jacek B. Gosk,[d] Roman Puźniak,[e] Jacques Pécaut,[bc] Vincent Maurel*[bc] and Irena Kulszewicz-Bajer*[a]

Received 4th May 2017,
Accepted 9th June 2017

DOI: 10.1039/c7tc01932g

rsc.li/materials-c

Arylamine moieties oxidized to radical cations are promising spin bearers for organic high-spin compounds. However, successive oxidations of next-neighbour sites as well as the resulting ferromagnetic exchange interactions depend strongly on the charge and spin distributions over the molecule. We report here that the use of rigid segments composed of *m*-phenylene spin couplers linked to arylamine spin bearers in a co-planar way facilitates successive oxidations, enhances spin exchange interactions and doubles the observed spin state (S = 2) in a polymer (PQA) when compared to the chemically equivalent (but locally free rotating) PA2 polymer (S = 1). Such a quintet spin state is observed for the first time for a linear polyarylamine with an *m*-phenylene coupler. DFT calculations of the dimer QA reproduce the experimental J value and indicate that oxidation of these co-planar compounds leads indeed to well localized radical cations, a fact of crucial importance for the preparation of arylamine-type high-spin materials.

Open Access Article. Published on 19 June 2017. Downloaded on 5/22/2026 2:47:09 AM.
This article is licensed under a Creative Commons Attribution 3.0 Unported Licence.

Introduction

Organic high-spin dimers, oligomers and polymers have been the object of intense research efforts for the last twenty years,[1–5] with the aim of obtaining materials useful for spintronics,[6] MRI contrast agents[7] or purely organic magnetic materials.[8] The most popular and versatile strategy to obtain high-spin organic materials is to connect π-conjugated free radicals acting as "spin bearers" *via* π-conjugated "spin couplers", the most documented example of which is the *m*-phenylene group.[1,2] Such spin couplers mediate ferromagnetic spin coupling following the theory of alternant hydrocarbons.[9] High-spin oligomers and polymers based on the *m*-phenylene spin coupler and arylamine radical cation spin bearers have been therefore extensively studied, due to the high stability of these spin bearers (up to room temperature).[10,11] However, the highest spin state obtained to date is S = 9/2 for highly branched and poorly processable polymers.[12] For the best linear polymer[13] the highest spin state was found to be S = 1 with the exchange coupling constant, J/k_B = 18 K (**PA2**, see Scheme 1).

An important factor that prevents the achievement of higher S and J values is that in most systems reported to date (like in **D2** and **PA2**, Scheme 1 and ref. 13), the phenyl rings of the spin couplers and spin bearers are not coplanar and therefore do not behave strictly as alternant hydrocarbons. A solution to this problem would be to prevent the rotation of the spin bearers around the $C_{coupler}$–N_{bearer} bond (*i.e.* the C–N bonds in the *meta* positions of the central *m*-phenyl group in **D2** or **QA**) by the insertion of an additional covalent link. Rajca and co-workers demonstrated the benefit of this last approach synthesizing fully rigid ladders of *m*-aniline oligomers[4,14] which were converted into neutral oligoaminyl radicals with high estimated J values and high spin up to S = 2 in the tetramer.[14]

Herein we report the synthesis and the characterization of partially rigid compounds **QA** and **PQA**, formally derived from the more "flexible" **D2** and **PA2** analogues (Scheme 1). This study aimed at examining the effect of such a local co-planarity between the spin coupler ring and the spin bearers on the redox properties, the maximum spin S observed and the exchange coupling constant. Notably, here are the main results: (i) the synthetic strategy of such semi-rigid compounds could be extended to the polymeric system like **PQA**, (ii) rather unexpectedly, the electrochemical properties of the semi-rigid **QA** and **PQA** compounds were more favourable than those of the flexible analogues, (iii) the magnetic properties of **QA** and **PQA** oxidized

[a] Faculty of Chemistry, Warsaw University of Technology, Noakowskiego 3, 00-664 Warsaw, Poland. E-mail: ikulsz@ch.pw.edu.pl
[b] INAC, SyMMES Université Grenoble Alpes, F-38000 Grenoble, France
[c] INAC, SyMMES, CEA Grenoble, F-38054 Grenoble, France
[d] Faculty of Physics, Warsaw University of Technology, Koszykowa 75, 00-662 Warsaw, Poland
[e] Institute of Physics, Polish Academy of Science, Al. Lotników 32/46, 02-668 Warsaw, Poland

† Electronic supplementary information (ESI) available. CCDC 1545978. For ESI and crystallographic data in CIF or other electronic format see DOI: 10.1039/c7tc01932g

Open Access Article. Published on 19 June 2017. Downloaded on 5/22/2026 2:47:09 AM.
This article is licensed under a Creative Commons Attribution 3.0 Unported Licence.

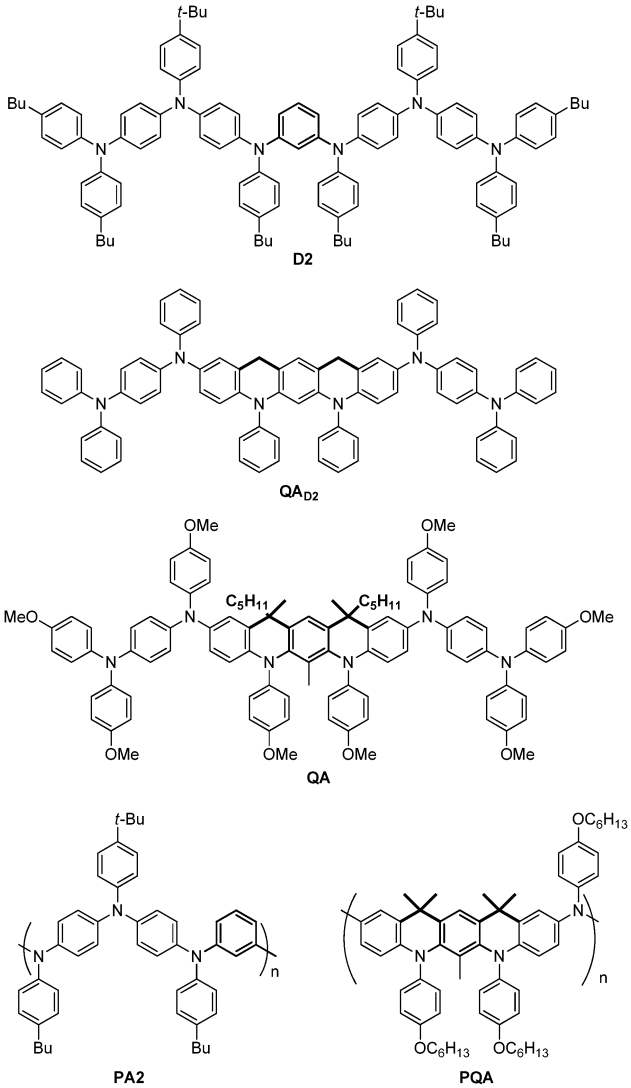

Scheme 1 The chemical structures of **QA** and **PQA** with a rigid coupler and their flexible analogues **D2** and **PA2**.

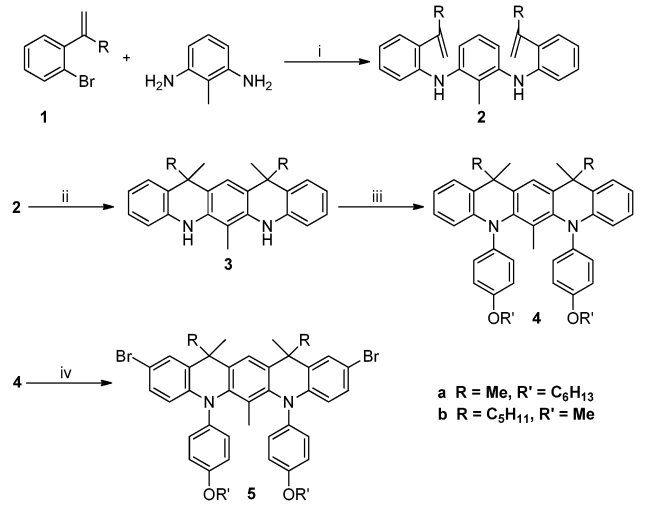

Scheme 2 Synthesis of intermediate bromides. Conditions: (i) **5a** 3% $[Pd_2(dba)_3]$, P(*t*-Bu)$_3$, *t*-BuONa, Ar, 110 °C, **5b** 3% $[Pd(OAc)_2]$, P(*t*-Bu)$_3$, *t*-BuONa, Ar, 120 °C; (ii) 85% H_3PO_4, $MeCO_2H$, Ar, 100 °C; (iii) 1-(hexyloxy)-4-iodobenzene (**7a**) or 4-iodoanisole (**7b**) 3–5% $[Pd(OAc)_2]$, P(*t*-Bu)$_3$, *t*-BuONa, Ar, 110 °C; (iv) NBS, DMF, Ar, 0 °C.

to radical cations (spin *S* value achieved, the magnetic exchange coupling constant for **PQA**) were significantly improved compared with those of **D2** and **PA2**, demonstrating the interest of introducing local co-planarity.

Results and discussion

Synthetic strategy

The model compound **QA** and its polymeric analogue, **PQA,** were synthesized in similar ways. The synthetic routes incorporated palladium catalysed Buchwald–Hartwig aminations combined with Sonogashira coupling and several classical organic transformations. As presented in Scheme 1, the main structural unit unifying **QA** and **PQA** is the 5,7,12,14-tetrahydroquinolino[3,2-*b*]-acridine core, which provides the planarization of the molecule and increases its rigidity. The complete synthetic pathway can be divided into two parts: the synthesis of intermediate bromides **5a** and **5b** (Scheme 2) and their further transformation into the title **QA** and **PQA** (Scheme 3). Thus bromides **1** (for the synthesis see the ESI†) were coupled with 2,6-diaminotoluene (used to avoid the unwanted cyclization direction in the next step) in Buchwald–Hartwig amination, catalysed by $Pd_2(dba)_3$/P(*t*-Bu)$_3$ (**2a**) or $Pd(OAc)_2$/P(*t*-Bu)$_3$ (**2b**). Then, both derivatives were subjected to cyclization, performed in a mixture of acetic acid and phosphoric acid. For the compound **3b** however, two possible diastereomers were possible to form: one *meso* (12*R*,14*S*) and two enantiomers: (12*S*,14*S*) and (12*R*,14*R*). Without subsequent separation of the diastereomers, any further step became significantly difficult due to small differences in chemical shifts and therefore lack of reliable product identification. Diastereomers could be separated by chromatography and then used in pure isomeric form (the respective, superimposed ^{1}H NMR spectra of diastereomers of **3b** are presented in Fig. S1, ESI†). The derivatives **3** containing secondary amine sites were transformed into tertiary amines *via* Buchwald–Hartwig amination giving compounds **4a** and **4b**, which upon treatment with NBS afforded the bromides **5a** and **5b**. One of the diastereomers of **5b** (the *meso* form) formed single crystals suitable for X-ray study. Based on the crystallographic data (Fig. S2, ESI†) we were able to assign the absolute configurations and differentiate the NMR spectra from Fig. S1 (ESI†) corresponding to the adequate diastereomeric form.

The model compound **QA** and corresponding **PQA** were synthesized as depicted in Scheme 3. **QA** was obtained *via* coupling of **5b** with amine **9** (the synthesis of **8** and **9** is shown in ESI,† Scheme S2) using the $Pd(OAc)_2$/P(*t*-Bu)$_3$ catalyst. The synthesis of **PQA** required the functionalization of **5a** with amine **8**, which upon reduction with ammonium formate resulted in the formation of amine **7**. The polycondensation of dibromoderivative **5a** with diamine **7** in the presence of $Pd(OAc)_2$/P(*t*-Bu)$_3$ yielded the polymer **PQA**. The polymer exhibited a weight-averaged molecular weight of 161 kDa and a number-averaged molecular weight of 497 kDa, M_w/M_n = 3.08.

Open Access Article. Published on 19 June 2017. Downloaded on 5/22/2026 2:47:09 AM.
This article is licensed under a Creative Commons Attribution 3.0 Unported Licence.

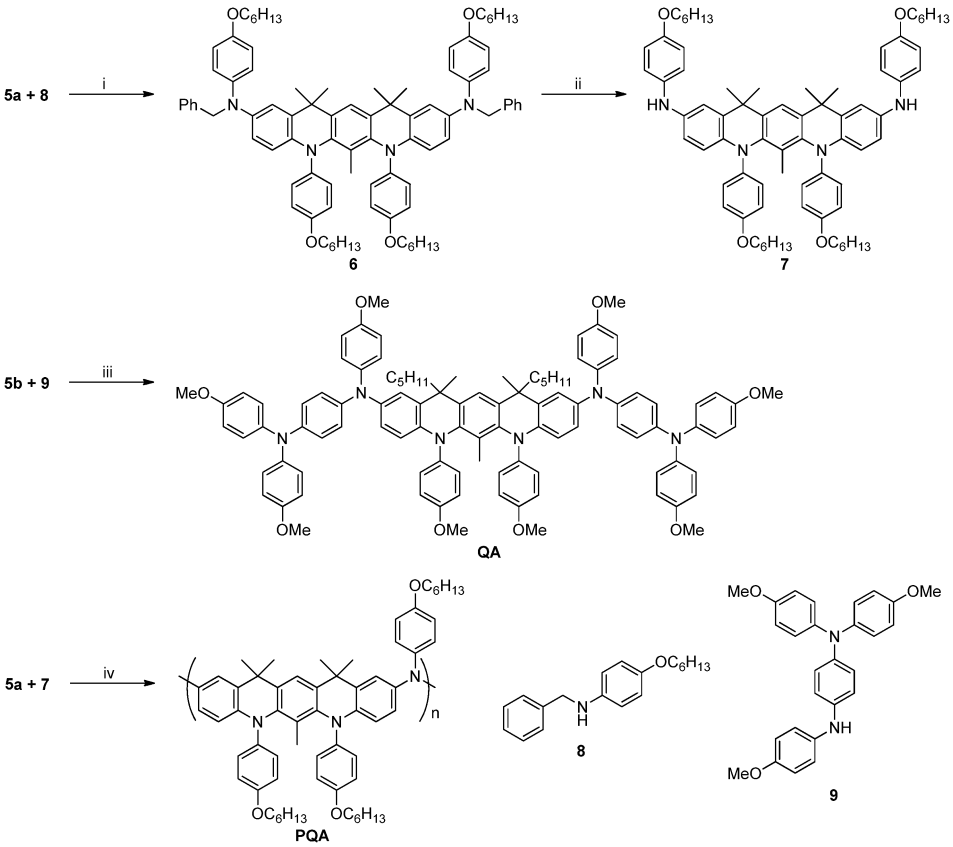

Scheme 3 Synthesis of the target dimer (QA) and polymer (PQA). Conditions: (i) 3% $[Pd(OAc)_2]$, $P(t\text{-}Bu)_3$, *t*-BuONa, Ar, 110 °C; (ii) HCO_2NH_4, 10% Pd/C, MeOH, Ar, reflux; (iii) 3% $[Pd(OAc)_2]$, $P(t\text{-}Bu)_3$, *t*-BuONa, Ar, 110 °C; (iv) 3% $[Pd(OAc)_2]$, $P(t\text{-}Bu)_3$, *t*-BuONa, Ar, 110 °C.

Electrochemical studies

The electrochemical oxidation of the dimer **QA** and the polymer **PQA** were studied by cyclic voltammetry and differential pulse voltammetry and their voltammograms are compared with previously reported voltammograms for **D2** and **PA2** in Fig. 1 (for the results of chemical oxidation followed by UV-vis-NIR spectroscopy see the ESI,† Section VI).

The voltammogram of **QA** showed two reversible waves at −0.125 V and 0.26 V (*vs.* Fc/Fc^+) independently of diastereisomeric forms (Fig. 1a). Both peaks were rather broad with $E_{ox} - E_{red}$ = 100 mV and 120 mV, respectively, suggesting that multi-electron oxidation processes took place in both cases. The first peak can be related to the formation of one radical cation within each arylamine conjugated segment separated *via* the *m*-phenylene coupler. By contrast, the oxidation of **D2** to one radical cation in each arylamine segment proceeded at higher potentials and in two steps (−0.09 V and −0.005 V *vs.* Fc/Fc^+) separated by a 85 mV shift. The second oxidation wave of **QA** can be attributed to the formation of a second radical cation within each conjugated segment.

Similar patterns were observed in the cyclic voltammogram of the polymer **PQA**, namely two broad reversible oxidation peaks were observed at 0.005 V and 0.34 V (*vs.* Fc/Fc^+, $E_{ox} - E_{red}$ = 140 mV and 190 mV, respectively) (Fig. 1b). Similar to the oxidation of **QA** these peaks correspond to the formation of one and then two radical cations per polymer unit. By contrast, the peaks corresponding to the first and the second one-electron oxidations in **PA2** were observed with a shift of 140 mV (E = −0.065 and 0.085 V) and correspond to the formation of radical cations in two adjacent mers (see ref. 13).

Normally, the redox potential increase can impede the creation of radical cations in adjacent units and this was identified as the main cause of unsuccessful attempts to obtain high-spin polyradical cations from oligo(*m*-aniline) derivatives.[15] Remarkably here, in terms of redox potentials, the use of the planar 5,7,12,14-tetrahydroquinolino[3,2-*b*]acridine core for both **QA** and **PQA** almost cancels the cost of oxidizing two arylamines connected by the *m*-phenylene spin coupler. This feature appears to be crucial for obtaining high-spin polymers with radical cation spin bearers.

This behaviour could be related to (i) the intrinsic favourable localization of the cationic charge after the first oxidation, and/or (ii) energetic compensation upon second oxidation (*via* local geometry constraint relaxation and/or rearrangement of the counter-anions and/or various interactions with the solvent, see ref. 16 for a review of such effects).

DFT calculations

As a preliminary way of exploring these possibilities, and for the sake of comparison, we first performed DFT calculations

Open Access Article. Published on 19 June 2017. Downloaded on 5/22/2026 2:47:09 AM.
This article is licensed under a Creative Commons Attribution 3.0 Unported Licence.

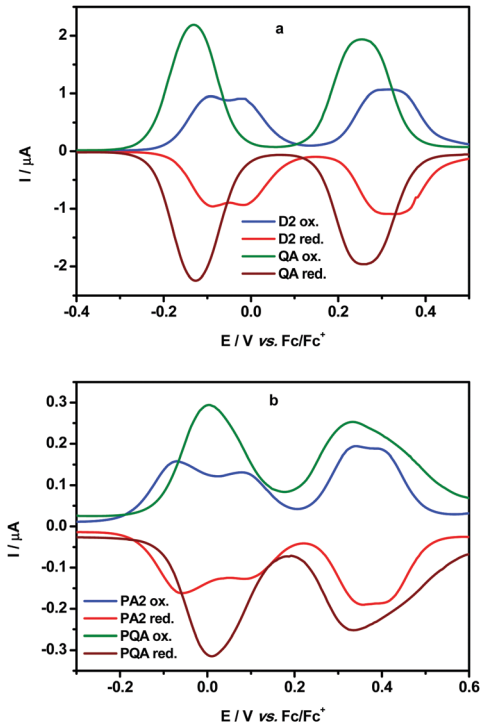

Fig. 1 Differential pulse voltammograms of dimers **QA** and **D2** (a) and of polymers **PQA** and **PA2** (b) in CH_2Cl_2 solution ($c = 1 \times 10^{-3}$ M) containing an electrolyte – 0.1 M Bu_4NBF_4 (modulation time 50 ms, modulation amplitude 10 mV, step potential 5 mV).

in vacuo on the mono-oxidized states of both **D2** and a **QA** model ($\mathbf{QA_{D2}}$) derived from **D2** only by adding two connecting CH_2 groups (see Scheme 1 above; the same procedure was then applied to a more suitable QA model: see below). Within an isotropic environment (*i.e.* without a counter-anion), the unpaired electron is artificially fully delocalized by DFT in both **D2** and $\mathbf{QA_{D2}}$ models (Fig. S12, ESI†). However, when placing sideways a negative charge mimicking the counter-anion, the topological difference between **D2** and $\mathbf{QA_{D2}}$ is manifested (see Fig. 2 and the ESI,† Fig. S13 for details). In $\mathbf{QA_{D2}}$, the alternant (conjugated) hydrocarbon theory is enforced by local planarity of the coupler and adjacent bearers. This results in complete lateralization of the cationic hole on one side of the dimer. By contrast, placing the same negative charge sideways, lateralization is only partly realized in **D2** because of non-planarity around the coupler leading to charge leakage between both sides (see Fig. 2 and Fig. S13, ESI†). The better localization of the charge in $\mathbf{QA_{D2}}$ compared with **D2** can explain, at least partially, the more favourable redox properties of **QA** reported above. To further validate these calculations, the *meta*-phenylene coupler in $\mathbf{QA_{D2}}$ was changed into a *para*-phenylene coupler. Consistent with the alternant hydrocarbon theory, no localization of the charge was observed in spite of the introduction of the same lateral negative charge (Fig. S14, ESI†). Finally, the same procedure was applied to a quasi-QA dimer, with its OMe moieties and $>CMe_2$ bridges ($\mathbf{QA_{CMe}}$), encompassing all the main features of QA. In the presence of the same lateral charge, its HOMO becomes strongly lateralized, as already observed in the case of $\mathbf{QA_{D2}}$ (Fig. 2, bottom left). This is

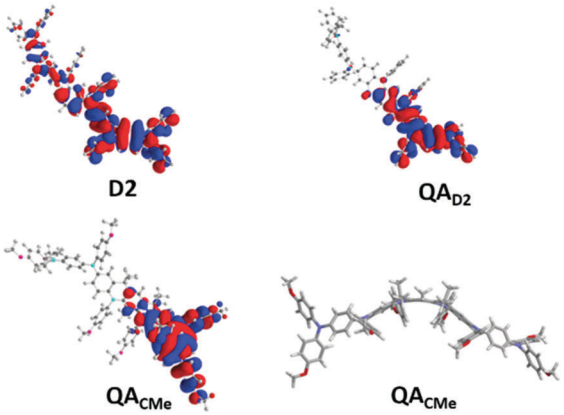

Fig. 2 HOMOs for the mono-oxidized redox state of **D2** (top left), $\mathbf{QA_{D2}}$ (top right) and $\mathbf{QA_{CMe}}$ (bottom left) in the presence of a lateral negative charge (see main text and the ESI† for details). Isodensity value: 0.01 a.u. Bottom right: Lateral view of $\mathbf{QA_{OMe}}$ showing bending of the molecular structure around the central coupler.

more remarkable as $\mathbf{QA_{CMe}}$ (and therefore QA) is actually slightly bent: the relative angle defined by the planes of the central (coupler) phenyl ring and of the adjacent (bearer) phenyl ring is 15°; the intersection of these planes occurs precisely at the level of the $>CMe$ bridges. Such a difference between ideal planarity (**D2** and $\mathbf{QA_{D2}}$) and the actual dimer ($\mathbf{QA_{CMe}}$) has here negligible (as observed experimentally) consequences for the redox properties.

EPR nutation and SQUID magnetometry studies

The magnetic interaction between the created spins was studied with pulsed EPR nutation spectroscopy (Fig. 3 and the ESI,† Section VII) and SQUID magnetometry (Fig. 4, 5 and ESI,† Section VIII). When **QA** was chemically oxidized to one radical cation per arylamine unit (using tris(4-bromophenyl) amminium hexachloroantimonate, TBA, see ESI,† Section IV), the EPR nutation spectrum of the frozen solution exhibited a very dominant signal at the $S = 1$ nutation frequency with a very small residual signal at the $S = 1/2$ frequency (Fig. 3). The magnetization data obtained by SQUID magnetometry (at $T = 2$ K) for samples oxidized to the same level, but after removal of the solvent, can be very

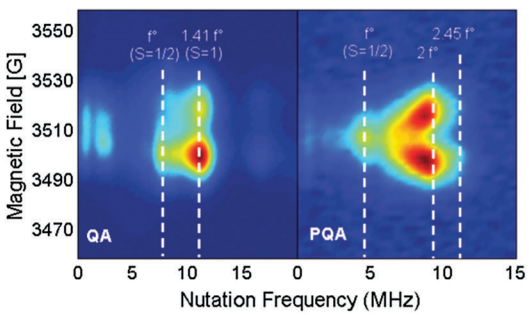

Fig. 3 EPR nutation spectra of **QA** and **PQA** ($T = 10$ K) oxidized with 1 eq. per arylamine unit. The microwave power was set so $f°(S = 1/2) = 7.7$ and 4.4 MHz for **QA** and **PQA** (respectively).

This journal is © The Royal Society of Chemistry 2017

Open Access Article. Published on 19 June 2017. Downloaded on 5/22/2026 2:47:09 AM.
This article is licensed under a Creative Commons Attribution 3.0 Unported Licence.

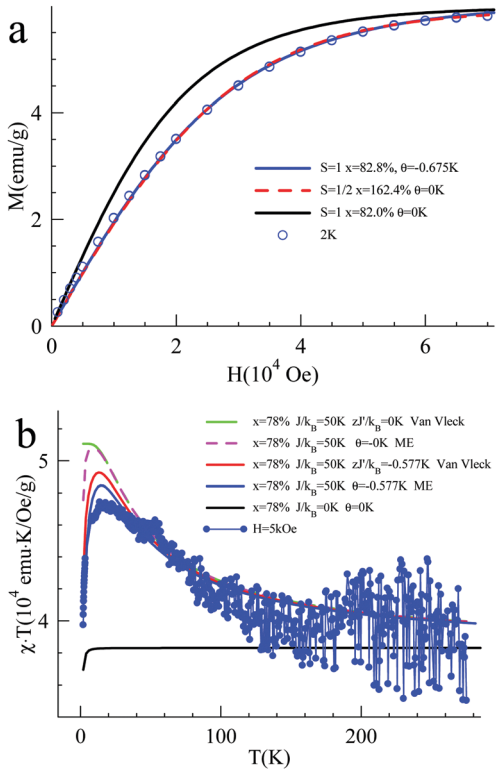

Fig. 4 (a) Magnetization of **QA** diluted in a polystyrene matrix (0.58%$_{mol}$) *versus* magnetic field at T = 2 K. (b) Product of magnetic susceptibility and temperature (χT) *vs.* temperature at H = 5000 Oe obtained for the **QA** sample diluted in a polystyrene matrix (see the ESI,† Section VIII for expression used for the Van Vleck eqn (S3) and the magnetization eqn (S4), derived from the Heisenberg exchange Hamiltonian).

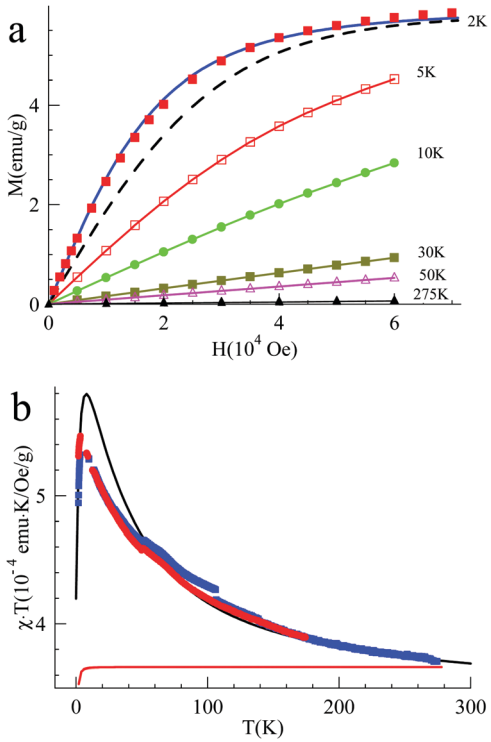

Fig. 5 (a) Magnetization of **PQA** *vs.* magnetic field (solid blue line – for S = 2, x = 23.5%, θ = −0.85 K; dashed black line – for S = 1/2, θ = 0 K). (b) The product of magnetic susceptibility and temperature *vs.* temperature at H = 0.5 × 10^4 Oe (red points) and at 10^4 Oe (blue points) for **PQA**. The black line corresponds to the numerical calculations of the eqn (S5) for x = 20%, θ = −1 K, J/k_B = 50 K (the four FM spin interaction/quintet state) while the red line represents non-interacting spins described by the standard Brillouin function with S = 1/2, x = 87.5%.

well fitted with the effective Brillouin function for S = 1 including mean-field correction (θ = −0.92 K) accounting for intermolecular antiferromagnetic interactions (the ESI,† Section VIII, Fig. S8). From this fit, it was also shown that 78% of **QA** dimers were in the triplet state expected for this oxidation stoichiometry. The product of magnetic susceptibility and temperature *versus* the temperature curve of the **QA** sample was dominated by intermolecular antiferromagnetic interaction (ESI,† Fig. S9), which impeded the measurement of the J exchange coupling constant within the diradical dication. To decrease such antiferromagnetic interactions, the **QA** dimer was diluted in a polystyrene matrix. The magnetization data *versus* magnetic field at T = 2 K were similar to the former one and confirmed the presence of S = 1 (Fig. 4a). The shape of χT *vs.* T (Fig. 4b) is now mainly due to the ferromagnetic interaction between both radical cations; the intramolecular coupling constant J/k_B was estimated to be *ca.* 50 K (*versus* the value of 35 K for **D2**).

When **PQA** was oxidized chemically to one radical cation per mer, the EPR nutation spectrum of the frozen solution exhibited a dominant signal at a nutation frequency close to $2{\cdot}f^{\circ}$ (f° being the S = 1/2 nutation frequency). Moreover, a smaller but clear signal can be observed up to $\sqrt{6}{\cdot}f^{\circ}$ (see Fig. 3). Such a spectrum is typical of S = 2 spin states[11,17,18] (see the ESI† for details) and demonstrates that S = 2 states were dominant at this oxidation stoichiometry. This spin multiplicity was thus twice that detected for the equivalent but flexible polymer **PA2**. Lower and higher oxidation stoichiometries lead to lower S values (see the ESI†). The magnetization measured as a function of magnetic field by SQUID magnetometry (at T = 2 K) for **PQA** samples oxidized in the best stoichiometry was very well fitted with the effective Brillouin function for S = 2 including mean-field correction (θ = −0.85 K) which reflects interchain antiferromagnetic interactions (Fig. 5a). From this fit it appears that *ca.* 90% mers of the **PQA** polymer contribute to the S = 2 state observed both by SQUID and by pulsed EPR nutation experiments. The χT *vs.* T plot rises up for decreasing temperature from 275 to 6 K and then decreases for temperatures approaching 2 K (Fig. 5b). The experimental curve reveals ferromagnetic interactions between spins along the polymer chain and antiferromagnetic ones between chains, which dominate at low temperatures. It should be emphasized that the polymer chains cannot be so closely packed as in the case of **QA** molecules, due to different local conformations, thus the χT curve allows for the detection of the ferromagnetic interaction even for solid state samples. The experimental data were approximated using the numerical solution of the Hamiltonian (S5) (see the ESI,† Section VIII) which leads to the exchange coupling constant J/k_B = 50 K, to be compared to a value of 18 K for the equivalent **PA2** polymer. The magnetic studies unequivocally confirm the formation of a quintet ground state in **PQA**, thus four spins in

Open Access Article. Published on 19 June 2017. Downloaded on 5/22/2026 2:47:09 AM.
This article is licensed under a Creative Commons Attribution 3.0 Unported Licence.

Table 1 Exchange coupling constants J/k_B computed for various dimers (**D2**, $\mathbf{QA_{D2}}$ and $\mathbf{QA_{CMe}}$ models) compared (when available) to the experimental values for dimers and polymers (**PA2** and **PQA**) (see Scheme 1, main text and ESI)

Molecules	D2	PA2	$\mathbf{QA_{D2}}$	$\mathbf{QA_{CMe}}$	PQA
J/k_B (DFT) (K)	35	—	116	42	—
J/k_B (exp.) (K)	35	18	—	~50	~50

adjacent mers of the polymer chain can be effectively coupled in a ferromagnetic fashion.

DFT calculations of exchange coupling constants

To compare the magnetic properties determined experimentally to those theoretically predicted by DFT, we considered the exchange coupling constant J/k_B for the various dimers (**D2**, $\mathbf{QA_{D2}}$ and $\mathbf{QA_{CMe}}$) already introduced above (see Scheme 1 and Fig. 2). For $\mathbf{QA_{D2}}$, we obtained a J/k_B value of 116 K, about three times larger than 35 K (both measured and computed) for **D2** (see Table 1). The incorporation of the methoxy OMe groups on the phenyl rings (compared to the simple $\mathbf{QA_{D2}}$) as well as the central (donor) methyl group to the *m*-phenylene spin coupler decreases however the value of J/k_B down to 42 K for $\mathbf{QA_{CMe}}$, close to the experimental value (50 K), also determined experimentally for **PQA**. Though somewhat disappointing, this last value is still three times higher than that measured for the analogous **D2** polymer (*i.e.* **PA2**): 18 K.[13] At this stage, the main reason that can be invoked to explain the J/k_B values' difference between $\mathbf{QA_{D2}}$ and $\mathbf{QA_{(CMe)}}$ has to do with the fact that the former one is strictly planar whereas the latter one is slightly bent (*cf.* the discussion about the redox properties). Following these observations, a more detailed DFT study of both substituent electronic effects and structural features on the magnitude of *J* coupling constants is currently underway and will be the subject of a specific theoretical publication.

Finally, it should be now emphasized that the doping efficiencies of **QA** and **PQA** (*ca.* 80–85% and *ca.* 90%, respectively) were distinctly higher than those of **D2** and **PA2** (65% and 66%, respectively). The high doping efficiencies of rigid compounds can be related to the formation of localized radical cations as evidenced by electrochemical and DFT studies. As a result, it increases the radical cation concentration.

Both effects (doping and redox) are important to minimize the number of spin defects which have a negative impact on spin coupling, especially in polymer chains. However, the most important question for us was to know how the insertion of additional bonds (*i.e. via* bridges) to prevent the relative rotation between spin bearers and a spin coupler would affect the spin multiplicity of **PQA** compared with the very limited spin multiplicity ($S = 1$) already reported for **PA2**. The EPR and magnetization studies showed that, for **PQA**, an almost pure quintet state ($S = 2$) was obtained with high doping efficiency. The presence of rigid, co-planar segments (*m*-phenylene coupler linked to adjacent spin bearers) most probably increases the overall stiffness of the chain, thus resulting in extended coil conformations. As it turns out, the ferromagnetic spin interaction can now be spread along the polymer chain up to four neighbouring units, related to the fact

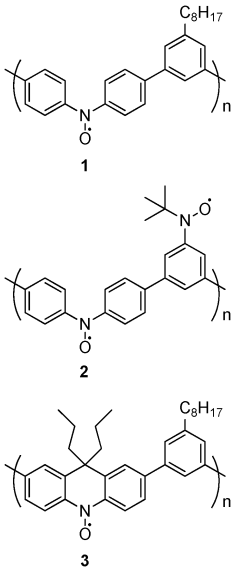

Scheme 4 The chemical structures of polynitroxides studied by Oka *et al.*[19]

that a twist of the geometry can now only take place at the central nitrogen atom of the spin bearers (a **PQA** mer possesses 2 – confined in the bearer – free bonds out of 6 bonds, whereas all 6 successive bonds are potentially free in a **PA2** mer). This constitutes progress as, to date, the presence of quintet spin states in linear polyarylamines was only detected for linear polymers with 3,4′-biphenyl couplers.[17] Remarkably, the coupling of four spins in **PQA** involves 8 free bonds (two per mer), whereas the coupling of four spins in the linear polymers **PB2** and **PB3** (see the ESI,† p. 53) with 3,4′-biphenyl couplers involves a very similar number of 9 free bonds (three per spin coupling unit). Similar trends were observed by Oka *et al.* for the polynitroxides **1**, **2** and **3** (Scheme 4).[19]

In the polynitroxide **1** each mer contains 4 bonds with free rotations around the nitroxide spin bearing unit, resulting in $S = 1$ spin state. In **3** one $>CPr_2$ bridge per mer is introduced and removes the free rotation of 2 bonds, yielding a $S = 3/2$ state. In the case of **1** and **3** polynitroxide, the increase of *S* (from 1 to 3/2) is probably less pronounced than that from **PA2** to **PQA** (from 1 to 2), because only 2 bonds out of 4 are immobilized for the polynitroxide instead of 4 bonds out of 6 for **PQA**. Moreover in the case of **PQA** all bonds around the *meta*-phenyl spin coupling moiety are blocked, which is more efficient than blocking only the bonds around the spin bearing NO° moiety in **3**.

Experimental section

For any experimental details on the chemical sources, synthesis, pulsed EPR and SQUID measurements as well as DFT calculations see the ESI.†

Conclusions

In summary, we demonstrated the efficient synthesis of the model compound (dimer) **QA** and of the polymer **PQA** with

 This journal is © The Royal Society of Chemistry 2017

Open Access Article. Published on 19 June 2017. Downloaded on 5/22/2026 2:47:09 AM.
This article is licensed under a Creative Commons Attribution 3.0 Unported Licence.

semi co-planar structures. The first two successive oxidations were observed without significant increase of the redox potential, which is crucial for obtaining high-spin arylamine materials and this can be rationalized by the formation of well localized radical cations. Though the presence of a co-planar structure around the spin couplers potentially leads to a significant increase of the ferromagnetic exchange coupling constant (*cf.* **D2** *versus* $\mathbf{QA_{D2}}$: Table 1), the slightly bent structure of **QA** (and, accordingly, of **PQA**) as well as the presence of the pending donor groups to stabilize the molecules upon oxidation, resulted in a relatively "small" magnitude of J/k_B. Still, this enabled an increase of the spin multiplicity in polymeric compounds: a quintet spin state ($S = 2$) was observed for the first time in the linear polymer **PQA** with an *m*-phenylene coupler. Moreover, the exchange coupling constant determined for **PQA** ($\sim$50 K) from magnetization measurements still showed a significant increase of the J/k_B value (*ca.* three times) in comparison to that estimated for the flexible analogue, **PA2** (18 K).

Acknowledgements

IKB and LS wish to acknowledge financial support from the National Science Centre in Poland (NCN, Grant No. 2015/17/B/ST5/00179). We acknowledge prof. Andrzej Twardowski and Anita Gardias for preliminary SQUID studies.

References

1 (*a*) P. Bujak, I. Kulszewicz-Bajer, M. Zagorska, V. Maurel, I. Wielgus and A. Pron, *Chem. Soc. Rev.*, 2013, **42**, 8895–8999; (*b*) A. Ito, D. Sakamaki, H. Ino, A. Taniguchi, Y. Hirao, K. Tanaka, K. Kanemoto and T. Kato, *Eur. J. Org. Chem.*, 2009, 4441–4450; (*c*) Y. Hirao, H. Ino, A. Ito, K. Tanaka and T. Kato, *J. Phys. Chem. A*, 2006, **110**, 4866–4872; (*d*) A. Ito, Y. Yamagishi, K. Fukui, S. Inoue, Y. Hirao, K. Furukawa, T. Kato and K. Tanaka, *Chem. Commun.*, 2008, 6573–6575; (*e*) A. Ito, K. Ota, K. Tanaka, T. Yamabe and K. Yoshizawa, *Macromolecules*, 1995, **28**, 5618–5625.

2 (*a*) J. A. Crayston, J. N. Devine and J. C. Walton, *Tetrahedron*, 2000, **56**, 7829–7857; (*b*) D. A. Dougherty, *Acc. Chem. Res.*, 1991, **24**, 88–94; (*c*) T. Sugawara, S. Murrata, K. Kimura, Y. Sugawara, H. Iwasaki and H. Iwamura, *J. Am. Chem. Soc.*, 1985, **107**, 5293–5394; (*d*) I. Fujita, Y. Teki, T. Takui, T. Kinoshita, K. Itoh, F. Miko, Y. Sawaki, H. Iwamura, A. Izuoka and T. Sugawara, *J. Am. Chem. Soc.*, 1990, **112**, 4074–4075.

3 (*a*) T. Aoki, T. Kaneko and M. Teraguchi, *Polymer*, 2006, **47**, 4867–4892; (*b*) T. Michinobu, J. Inui and H. Nishide, *Polym. J.*, 2010, **42**, 575–582; (*c*) D. Sakamaki, A. Ito, K. Tanaka, K. Furukawa, T. Kato and M. Shiro, *Angew. Chem., Int. Ed.*, 2012, **51**, 8281–8285; (*d*) D. Sakamaki, A. Ito, A. Furukawa, T. Kato, M. Shiro and K. Tanaka, *Angew. Chem., Int. Ed.*, 2012, **51**, 12776–12781; (*e*) Y. Yokoyama, D. Sakamaki, A. Ito, K. Tanaka and M. Shiro, *Angew. Chem., Int. Ed.*, 2012, **51**, 9403–9406.

4 (*a*) N. M. Gallagher, A. Olankitwanit and A. Rajca, *J. Org. Chem.*, 2015, **80**, 1291–1298; (*b*) A. Rajca, K. Shiraishi, M. Pink and S. Rajca, *J. Am. Chem. Soc.*, 2007, **129**, 7232–7233; (*c*) A. Rajca, *Chem. Rev.*, 1994, **94**, 871–893; (*d*) A. Rajca, S. Rajca and J. Wongsriratanakul, *J. Am. Chem. Soc.*, 1999, **121**, 6308–6309; (*e*) A. Rajca, J. Wongsriratanakul and S. Rajca, *J. Am. Chem. Soc.*, 2004, **126**, 6608–6626; (*f*) S. Rajca, A. Rajca, J. Wongsriratanakul, P. Butler and S. M. Choi, *J. Am. Chem. Soc.*, 2004, **126**, 6972–6986.

5 A. Rajca, *Chem. – Eur. J.*, 2002, **8**, 4834–4841.

6 T. Sugawara, H. Komatsu and K. Suzuki, *Chem. Soc. Rev.*, 2011, **40**, 3105–3118.

7 A. Rajca, Y. Wang, M. Boska, J. T. Paletta, A. Olankitwanit, M. A. Swanson, D. G. Mitchell, S. S. Eaton, G. R. Eaton and S. Rajca, *J. Am. Chem. Soc.*, 2012, **134**, 15724–15727.

8 A. Rajca, J. Wongsriratanakul and S. Rajca, *Science*, 2001, **294**, 1503–1505.

9 (*a*) A. A. Ovchinnikov, *Theor. Chim. Acta*, 1978, **47**, 297–304; (*b*) R. J. Bushby, D. R. McGill, K. M. Ng and N. Taylor, *J. Chem. Soc., Perkin Trans. 2*, 1997, 1405–1414; (*c*) R. J. Bushby, N. Taylor and R. A. Williams, *J. Mater. Chem.*, 2007, **17**, 955–964; (*d*) T. D. Selby, K. R. Stickley and S. C. Blackstock, *Org. Lett.*, 2000, **2**, 171–174; (*e*) E. Fukuzaki and H. Nishide, *Org. Lett.*, 2006, **8**, 1835–1838.

10 R. J. Bushby, D. Gooding and M. E. Vale, *Philos. Trans. R. Soc., A*, 1999, **357**, 2939–2957.

11 E. Dobrzynska, M. Jouni, P. Gawrys, S. Gambarelli, J. M. Mouesca, D. Djurado, L. Dubois, I. Wielgus, V. Maurel and I. Kulszewicz-Bajer, *J. Phys. Chem. B*, 2012, **116**, 14968–14978.

12 T. Michinobu, J. Inui and H. Nishide, *Org. Lett.*, 2003, **5**, 2165–2168.

13 V. Maurel, M. Jouni, P. Baran, N. Onofrio, S. Gambarelli, J. M. Mouesca, D. Djurado, L. Dubois, J. F. Jacquot, G. Desfonds and I. Kulszewicz-Bajer, *Phys. Chem. Chem. Phys.*, 2012, **14**, 1399–1407.

14 A. Rajca, A. Olankitwanit, Y. Wang, P. J. Boratynski, M. Pink and S. Rajca, *J. Am. Chem. Soc.*, 2013, **135**, 18205–18215.

15 R. J. Bushby, C. A. Kilner, N. Taylor and M. E. Vale, *Tetrahedron*, 2007, **63**, 11458–11466.

16 R. F. Winter, *Organometallics*, 2014, **33**, 4517–4536.

17 L. Skorka, J. M. Mouesca, L. Dubois, E. Szewczyk, I. Wielgus, V. Maurel and I. Kulszewicz-Bajer, *J. Phys. Chem. B*, 2015, **119**, 13462–13471.

18 A. Schweiger and G. Jeschke, *Principles of Pulsed Electron Paramagnetic Resonance*, Oxford University Press, Oxford, 2001.

19 (*a*) H. Oka, Y. Kiyohara, H. Kouno and H. Tanaka, *Polyhedron*, 2007, **26**, 2059–2064; (*b*) H. Oka, H. Kouno and H. Tanaka, *J. Mater. Chem.*, 2007, **17**, 1209–1215.